

## Effect of composition on the sintering and microstructure of diphasic mullite gels

Jian Yu <sup>a,\*</sup>, Jian-Lin Shi <sup>a</sup>, Qi-Ming Yuan <sup>b</sup>, Zheng-Fang Yang <sup>b</sup>, Yu-Ru Chen <sup>b</sup>

<sup>a</sup>The State Key Laboratory on High Performance Ceramics and Superfine Microstructure, Shanghai Institute of Ceramics, Chinese Academy of Sciences, 1295 Ding-xi Road, Shanghai 200050, PR China

<sup>b</sup>Department of Materials Science and Engineering, Tianjin University, Tianjin 300072, PR China

Received 21 February 1999; received in revised form 1 April 1999; accepted 24 May 1999

### Abstract

Diphasic gels with alumina/silica ratio of 68/32, 71.8/28.2, 74/26, and 76/24 were prepared and used to study the effect of the precursor composition on the mullite formation process, densification behavior, and microstructure development. Alumina contents of mullites in the samples sintered at high temperature (1650°C) for 4 h or at low temperature (1550°C) for longer time increased with the increase in alumina/silica ratio of the gels. A sharp decrease in densification rate was observed on transition from the mullite + silica-rich liquid phase field to the mullite solid solution. This decrease was associated with elimination of the viscous flow of the amorphous silica phase. However, the densification rate was higher for the samples with excess alumina than for the 74/26 sample. Both in the silica-rich sample (68/32) and the stoichiometric mullite sample (71.8/28.2), elongated mullite grains were observed. Such elongated grains grew at the expense of the surrounding smaller mullite grains. In the 74/26 and 76/24 samples, mullite grains were equiaxed. Furthermore, in the latter, elongated  $\alpha$ -Al<sub>2</sub>O<sub>3</sub> grains were observed. © 2000 Elsevier Science Ltd and Techna S.r.l. All rights reserved.

**Keywords:** A. Sol–gel processes; A. Sintering; D. Mullite

### 1. Introduction

Mullite has been recognized as an important structural, electronic, and optical material because of its excellent high temperature strength, creep resistance, good chemical and thermal stability, low thermal expansion coefficient, good dielectric and infrared transparency [1–4]. To enhance the performance of mullite, it is necessary to tailor the microstructure of the material to application. For instance, interlocked acicular grains may be best when creep resistance is desired [2]. However, fine equiaxed grains are most desired for good IR transparency and/or high room-temperature strength.

Several authors have demonstrated that sol–gel process can be designed to control the degree of alumina–silica mixing and, consequently, control mullite crystallization kinetics, densification and microstructure evolution [5]. While a sol–gel polymeric mixture resulted in the

equiaxed microstructure, variations in local chemical heterogeneity in a sol–gel colloidal (diphasic) mixture lead to anisotropic mullite grains at the same composition (72 wt% Al<sub>2</sub>O<sub>3</sub>) [5]. Another way to control microstructure evolution is to add seeds into the precursor material. Mroz and Laughner [6] reported that a dense, equiaxed grain structure could be developed at a relatively high seed concentration, whereas highly anisotropic, large grains dispersed in a matrix of small, equiaxed grains were obtained at a low seed concentration. Hong et al. [7] obtained largest anisotropic grains with a system seeded with 2 wt% mullite whiskers and doped with 2 wt% B<sub>2</sub>O<sub>3</sub>. A number of dopants such as B<sub>2</sub>O<sub>3</sub>, Fe<sub>2</sub>O<sub>3</sub>, and TiO<sub>2</sub> have been reported to promote anisotropic grain growth in mullite [7–9]. The anisotropic microstructure development [8,9] is attributed to a low glass viscosity in transition metal (titanium, iron) oxide-doped mullite and therefore the higher mobility of the diffusing species in glass.

Some authors [4, 10–14] have studied microstructural development of aluminosilicates with compositions near the single-phase mullite region. Equiaxed grains in

\* Corresponding author.

E-mail address: jianyu@goumai.sh.cn (J. Yu).

alumina-rich mullite is attributed to the kinetic limitation of material transport by solid-state diffusion whereas the presence of a liquid phase has been suggested to facilitate the growth of anisotropic grains in silica-rich mullites [13] (i.e. < 74 wt%  $\text{Al}_2\text{O}_3$ ). There are two possible mechanisms to explain the change of the growth process of mullite with composition. One of these mechanisms assumed that intrinsic growth rates of mullite crystals along different axes are always anisotropic

[8]. Mullite grains have therefore a strong tendency to grow as rods if the grains grow without constraint, such as in directional solidification [15] and during vapor–solid synthesis of whiskers [16]. The other mechanism assumes that the intrinsic growth rates are a function of composition, and a composition near the stoichiometric mixture promotes the growth along the  $c$  axis and/or suppresses the growth along the  $a$  and  $b$  axes [13]. Since no long-range diffusion is required in diphasic gels,

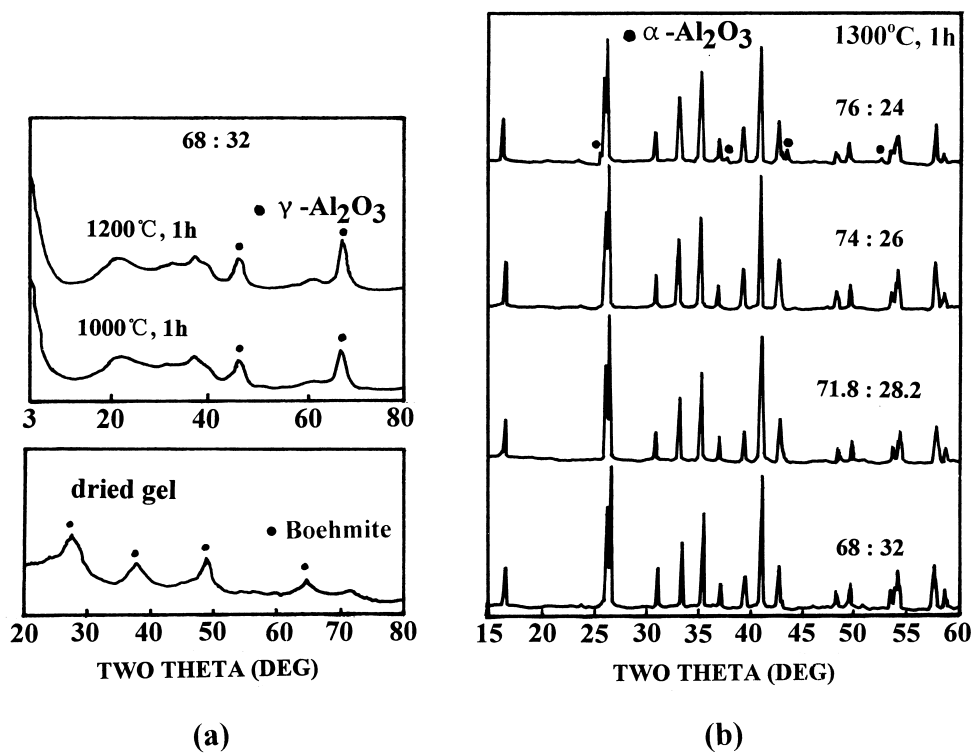


Fig. 1. XRD patterns for (a) the 68/32 gel, oven cooled from calcined temperatures; (b) the samples 68/32, 71.8/28.2, 74/26, 76/24, calcined at 1300°C for 1 h.

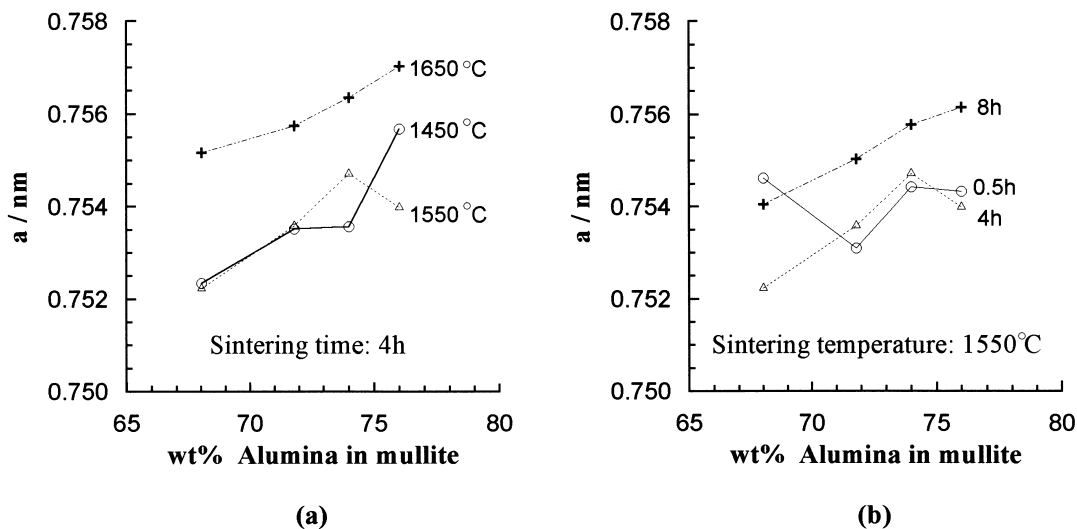


Fig. 2. Mullite lattice parameter  $a$  vs total alumina content in samples.

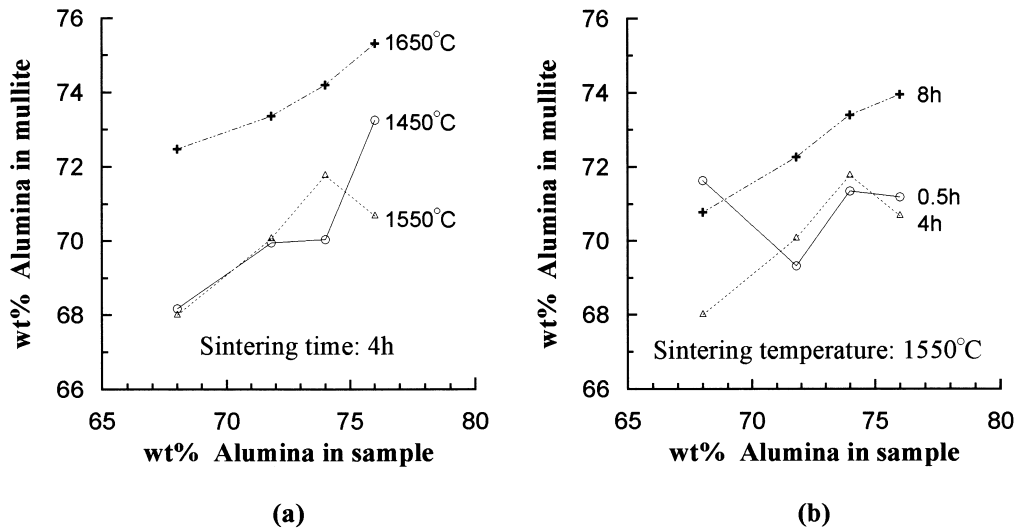


Fig. 3. Relation between alumina content in mullite and total alumina content in samples.

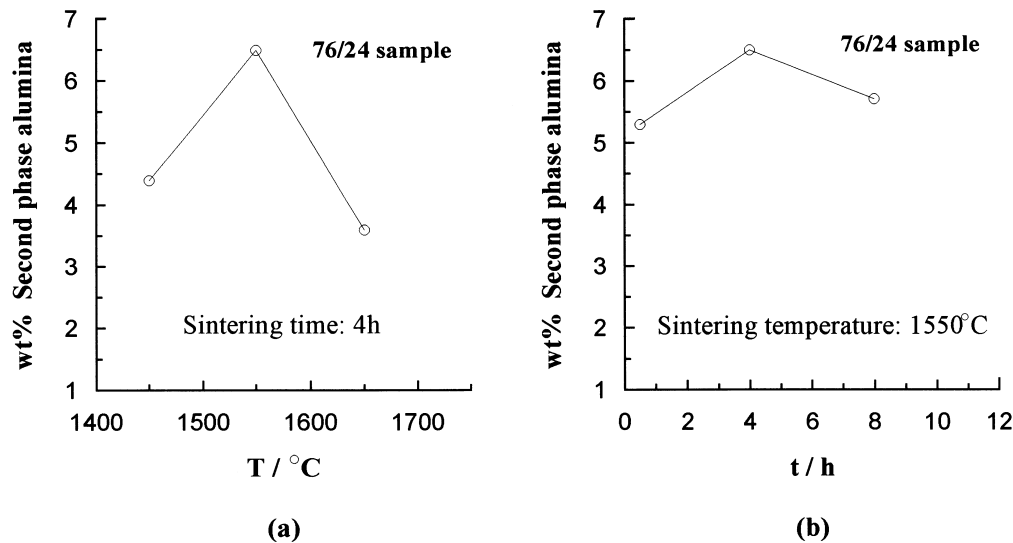


Fig. 4. Relation between second phase content ( $\alpha$ - $\text{Al}_2\text{O}_3$ ) in the 76/24 sample and sintering temperature (a), and sintering time (b).

which have nanometer-scale mixing, mullite grain morphology is determined by the intrinsic growth rates, which are limited by the short range diffusion.

In the diphasic mullite system, it is known that densification is aided by viscous flow of the amorphous silica phase and that this glass phase also enhances the development of anisotropic grains. Although there were many earlier studies [3, 5–8, 12–14, 17–21] that addressed the subject of densification and microstructure evolution in diphasic-gel-derived mullite, the effect of composition of diphasic mullite gels on the sintering and microstructure development were not systematically characterized. In this paper, sintering behavior and microstructure evolution of diphasic mullite gels were studied over a range of chemical compositions ( $\text{Al}_2\text{O}_3/\text{SiO}_2$  ratio).

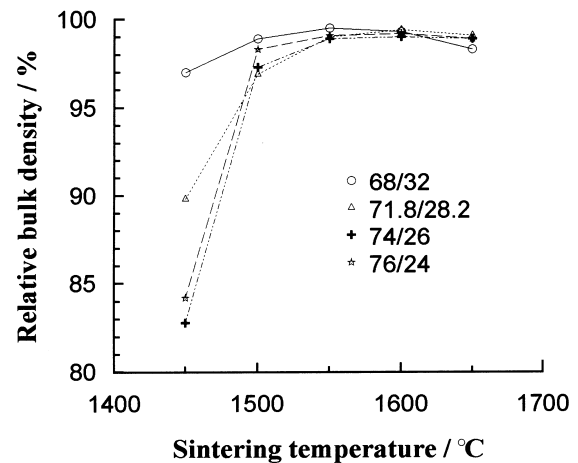


Fig. 5. Change in relative sintered density with sintering temperature (sintering time is 4 h).

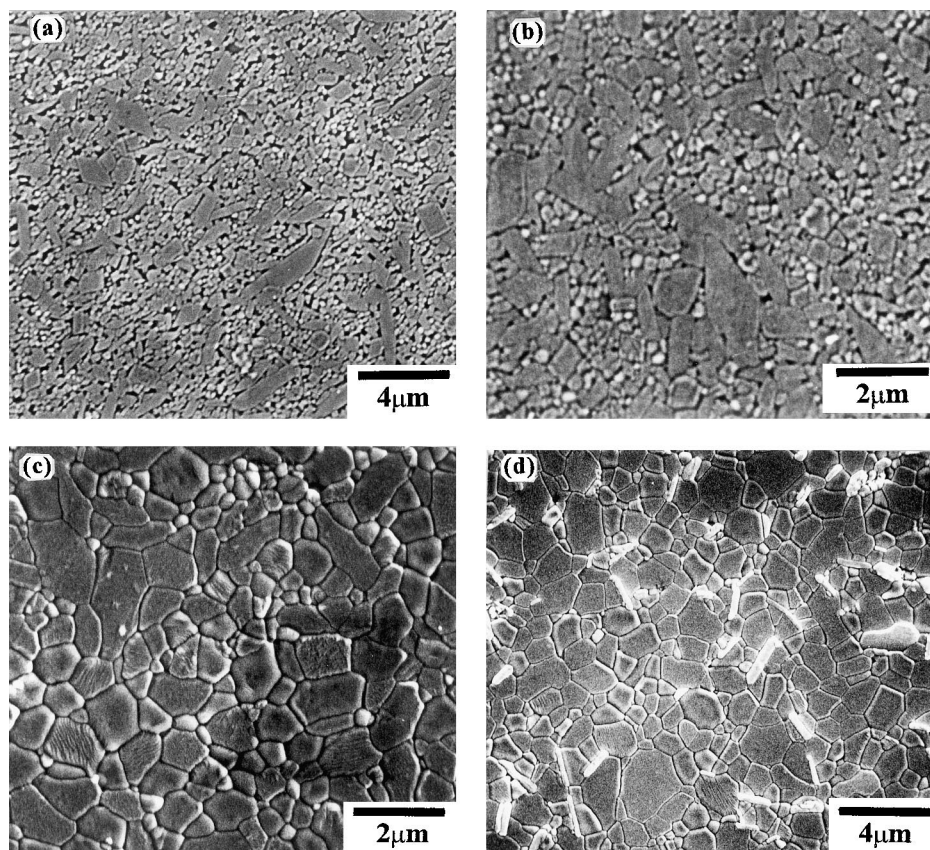


Fig. 6. Scanning electron micrographs of the samples (a) 68/32, (b) 71.8/28.2, (c) 74/26, and (d) 76/24, sintered at 1550°C for 4 h. Dark grains: mullite; light grains:  $\alpha$ -Al<sub>2</sub>O<sub>3</sub>.

## 2. Experimental procedure

Aluminum chloride and tetraethylorthosilicate (TEOS) were used to prepare diphasic mullite gels that had overall alumina/silica weight ratio of  $\sim 68/32$ ,  $\sim 71.8/28.2$ ,  $\sim 74/26$ , and  $\sim 76/24$  after heat treatment at 1600°C. At this temperature, equilibrium Al<sub>2</sub>O<sub>3</sub>-SiO<sub>2</sub> phase diagrams [22–25] indicate that “6832” samples are in the mullite + silica-rich liquid phase field, the “71.8/28.2” samples are stoichiometric mullite, the “74/28” samples are near the boundary between the mullite (solid solution) and mullite–alumina phase fields, and the “76/24” samples are in the mullite + alumina phase field.

A typical procedure for synthesis of the diphasic mullite gels is outlined as follows: A required amount of aluminum chloride was first dissolved in distilled water. High-purity TEOS, ethanol, and H<sub>2</sub>O with 0.018N HCl were mixed together in a ratio of 50 wt%:30 wt%:20 wt%. After the mixture was aged in a 70°C water bath for 1 h, the alumina solution was introduced, and mixed further for 1 h. Then the pH value of the mixture was increased to 8.5 by the addition of 3N NH<sub>3</sub>·H<sub>2</sub>O and aged in the same bath again for 3 h. The materials were filtered, washed thoroughly with distilled water, and

then dried at 100°C overnight. Gels obtained were calcined at 1000°C for 1 h, milled for 2 h to break up agglomerates in a Teflon-lined container using mullite balls, and subsequently isostatically pressed at 250 MPa. The green compacts obtained were sintered at various temperatures for different time periods.

X-ray diffraction (XRD) techniques were used for the phase identification of gel powders which were calcined at different temperatures, up to 1300°C. The sintered samples were ground and also analyzed by XRD using CuK $\alpha$  radiation with automatic divergence slit. The  $2\theta$  positions of six silicon peaks were used to correct  $2\theta$  positions for the samples, based on standard positions for the silicon peaks. Lattice parameters of mullite were calculated by the least-squares method using a computer program, selecting 11 XRD peaks ( $2\theta$  between 16° and 70°) nonoverlapping with Al<sub>2</sub>O<sub>3</sub> peaks, and using a step-wise scanning mode. The amount of  $\alpha$ -Al<sub>2</sub>O<sub>3</sub> was determined from the peak area ratio of the (113)  $\alpha$ -Al<sub>2</sub>O<sub>3</sub> reflection to the four mullite peaks (201, 121, 211, 230), as described by Klug et al. [25]. Sintered bulk densities were measured by the Archimedes method. The microstructure of the fully dense specimens was observed by scanning electron microscopy (SEM) on polished and thermally etched samples.

### 3. Results and discussion

According to previous studies [26–29], the mullite formation reaction in diphasic gels takes place between amorphous silica and transition alumina. This phenomenon is also observed in the present study (Fig. 1). The as-prepared gel had a structure of boehmite which changed after heating at  $T \approx 1000 \sim 1200^\circ\text{C}$  into a structure of  $\gamma\text{-Al}_2\text{O}_3$  or spinel [25, 26] and finally, crystallized into mullite at  $T \geq 1300^\circ\text{C}$ . In addition to mullite, a trace of  $\alpha\text{-Al}_2\text{O}_3$  was present in rich-alumina 76/24 samples. In rich-silica 68/32 samples, however, no crystalline silica phases were detected by XRD in any of the diphasic gels during heating. The only crystalline phase detected in the 68/32, 71.8/28.2, and 74/26 samples was mullite.

The change in the mullite lattice parameter  $a$  in the samples sintered at various temperatures for different times as a function of composition is depicted in Fig. 2. As can be seen from the figure, this parameter increased with the increase in the alumina/silica ratio of diphasic gels in the samples only sintered at  $1650^\circ\text{C}$  for 4 h and/or at  $1550^\circ\text{C}$  for 8 h. For the samples sintered at  $1550^\circ\text{C}$  for 4 h, the value of lattice parameter  $a$  was lower in the 76/24 sample than that in the 74/26 sample [Fig. 2(a)]. For the samples sintered at the same temperature for 0.5

h, this parameter was higher in the 68/32 sample than that in the stoichiometric samples [Fig. 2(b)]. Furthermore, for the 76/24 samples, the lattice parameter,  $a$ , was higher at  $1450^\circ\text{C}$  than at  $1550^\circ\text{C}$  [Fig. 2(a)], and was higher at  $1550^\circ\text{C}$  for 0.5 h than for 4 h [Fig. 2(b)]. The change in the parameter  $a$  with temperature or time was also similar to that observed in the 68/32 samples. These results, which have been related to the formation of a transient  $\text{Al}_2\text{O}_3$ -rich mullite just after crystallization, are in agreement with other authors (observation [13, 21]).

Because the plot of the  $a$  constant versus the  $\text{Al}_2\text{O}_3$  content gives a linear relationship, the plot has frequently been used to determine the alumina contents in mullite [30]. Fig. 3 shows alumina contents in mullite grain plotted against alumina contents in the samples. The alumina contents in mullite were determined from  $a$ -lattice parameters utilizing the curve given by Klug et al. [25]. In the samples within the single-phase mullite region (the 71.8/28.2 and 74/26 samples), the alumina contents in mullite became higher with increasing temperature. However, in the samples with excess silica or alumina relative to the mullite compositions in the solid-solution range, an alumina-rich mullite was initially formed. For instance, a kind of mullite with a composition

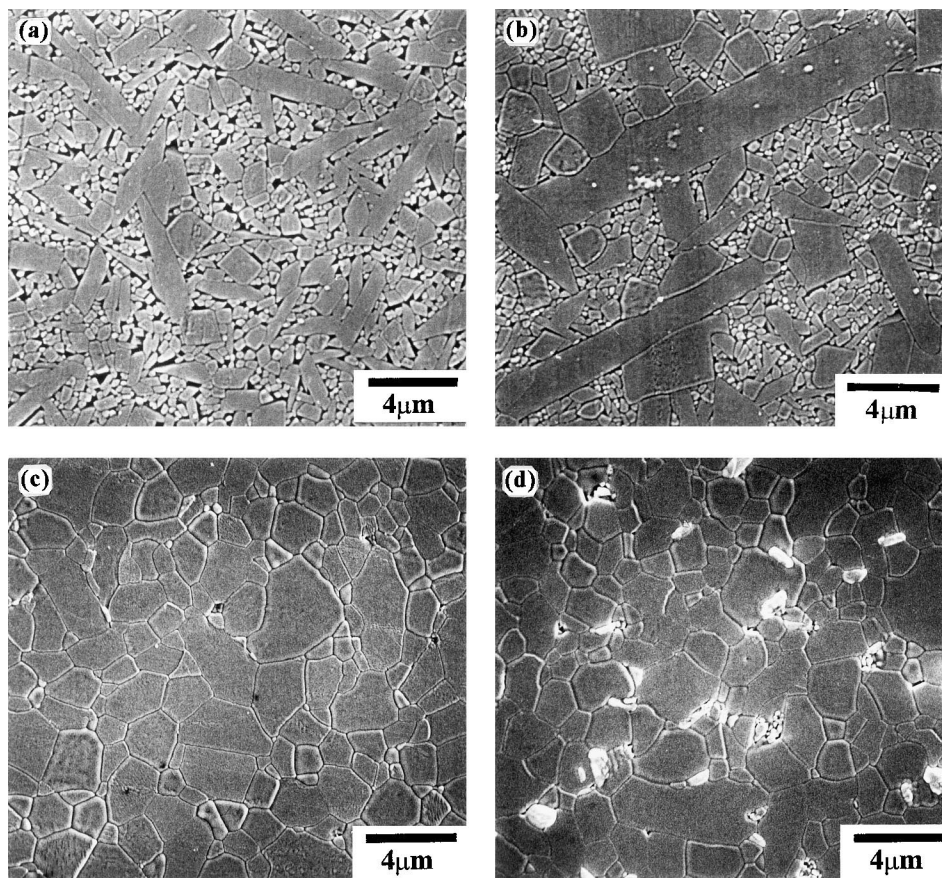


Fig. 7. Scanning electron micrographs of the samples (a) 68/32, (b) 71.8/28.2, (c) 74/26, and (d) 76/24, sintered at  $1550^\circ\text{C}$  for 8 h. Dark grains: mullite; light grains:  $\alpha\text{-Al}_2\text{O}_3$ .

of 73.3 wt% alumina was obtained in the 76/24 sample sintered at 1450°C for 4 h [Fig. 3(a)]. Further heating up to 1550°C decreased the amount of alumina in solid solution to 70.7 wt%, and subsequent treatments at higher temperature (1650°C) increased the amount of alumina to 75.3 wt%, which is near the overall composition and higher than the equilibrium composition predicted by Klug et al.'s phase equilibrium diagram [25]. The change in alumina contents of mullites in the 76/24 samples sintered at 1550°C with sintering time was similar [Fig. 3(b)]. The amount of alumina in mullite was higher for 0.5 h than for 4 h, longer treatments at this temperature (8 h) raised it to levels of 73.9 wt%. Samples with relatively low bulk alumina contents (the 68/32, 71.8/28.2, and 74/26 samples) had only mullite as the crystalline phase, while the alumina-rich sample (the 76/24 samples) contained some additional  $\alpha$ -Al<sub>2</sub>O<sub>3</sub> as secondary crystalline phase (Fig. 3). The content of  $\alpha$ -Al<sub>2</sub>O<sub>3</sub> reached its maximum value of 6.5 wt% for the 1550°C treatment and then decreased with increasing temperature [Fig. 4(a)]. At 1550°C, the content of second phase reached a maximum for 4 h treatment and then decreased with increasing time. The change in the content of  $\alpha$ -Al<sub>2</sub>O<sub>3</sub> in the 76/24 sample coincided with the change in the alumina content in mullite grain (Fig. 3).

The dependence of the sintered density on sintering temperature is shown in Fig. 5. The fired densities of the samples at 1450°C were below 90%TD for all compositions, with the exception of the 68/32 sample which reached 97%TD. The relative density for all compositions increased with increasing sintering temperature. Almost full densification >97%TD was reached at 1500°C for all samples. Because the precursor powders were calcined at 1000°C, an amorphous phase remained in the calcined powders and promoted densification by a transient viscous sintering mechanism. As the alumina/silica ratio increased, the relative density of the samples became lower. However, a closer look at the relative densities of the different samples shows that the relative density of the alumina-rich 76/24 sample was higher than that the 74/26 sample. These results are in agreement with those reported by Sacks [11] who indicated that in addition to the amorphous phase, other factors have important effects on the densification behavior of diphasic gels. In a compound with a solid solution range, the densification kinetics may be modified if changes in defect concentration of the slower diffusing species occur when the composition is altered. This does not appear to be an important factor in the present study since alumina content of mullite in the 76/24

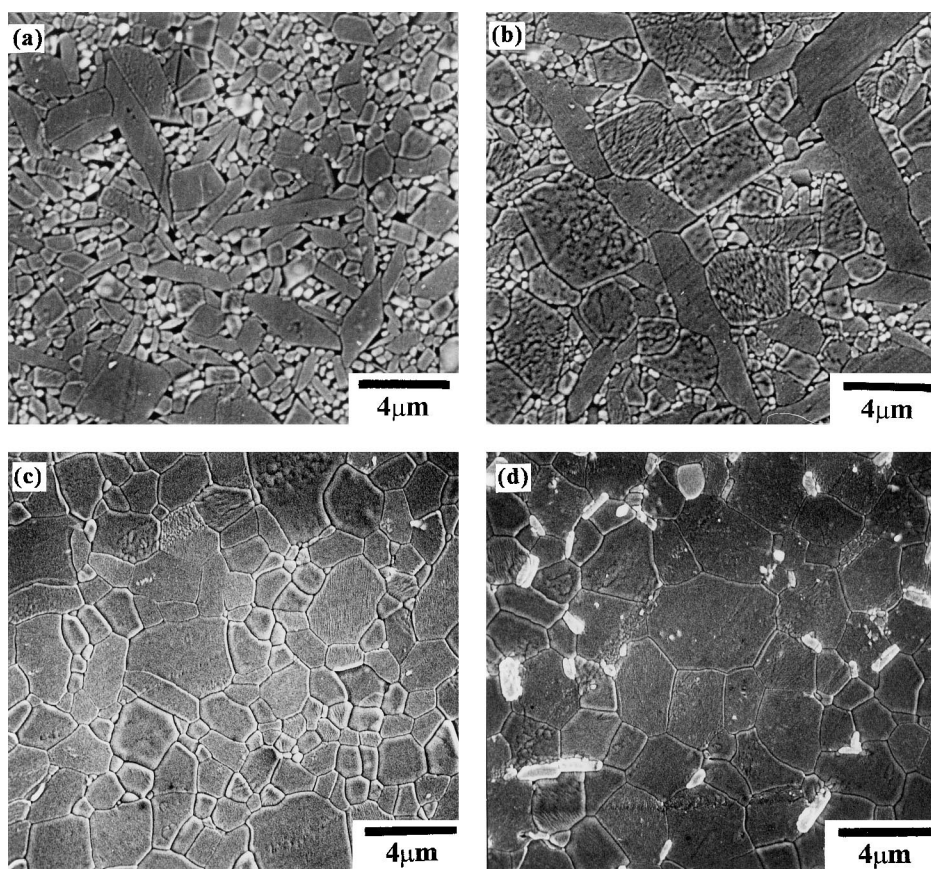


Fig. 8. Scanning electron micrographs of the samples (a) 68/32, (b) 71.8/28.2, (c) 74/26, and (d) 76/24, sintered at 1600°C for 4 h. Dark grains: mullite; light grains:  $\alpha$ -Al<sub>2</sub>O<sub>3</sub>.

sample during sintering was not always higher than that in the 74/26 sample. For example, alumina content of mullite was 70.7 wt% in the 76/24 sample sintered 1550°C for 4 h while 71.8 wt% in the 74/26 sample [Fig. 3(a)].

The relative density of the 68/32 sample reached a maximum of ~99% at 1550°C and then decreased with increasing sintering temperature. However, the relative densities of the 71.8/28.2, 74/26, and 76/24 samples reached their maximum value at 1600°C and then decreased with increasing sintering temperature. Based on a comparison of the densities and microstructures in this study, the density decrease coincided with the anisotropic grain growth. Density decreases after prolonged heating of mullite at high temperature have been attributed to exaggerated grain growth [8, 19, 31]. This suggests that the process of anisotropic grain growth might be responsible for densification.

Microstructures developed at 1550~1650°C were observed with SEM. Fig. 6 shows micrographs of polished and thermally etched sections for the samples sintered in air at 1550°C for 4 h. Both 68/32 and 71.8/28.2 samples have similar microstructures which consisted of some acicular and rectangular mullite grains in

a matrix of fine equiaxed mullite grains. Small proportion of elongated grains and rectangular grains implies that there were liquid phase along grains boundaries during sintering because these grains can only grow in the presence of a liquid phase [11]. Only equiaxed mullite grains were present in the 74/26 sample, while elongated  $\alpha$ -Al<sub>2</sub>O<sub>3</sub> grains, in addition to equiaxed mullite grains, were observed in 76/24 samples. Alumina grains were not observed in the 68/32, 71.8/28.2, and 74/32 samples (Fig. 6), since these samples are within the mullite + silica-rich liquid phase field or in the stable region of mullite solid solutions. When sintering time was increased to 8 h, as can be found in Fig. 7, large elongated grains and rectangular grains formed in the 68/32 and 71.8/28.2 samples and the aspect ratio of elongated grains increased with the increase in soaking time, even though the surrounding equiaxed grains remained almost unchanged. However, the aspect ratio of the  $\alpha$ -Al<sub>2</sub>O<sub>3</sub> in the 76/24 sample is still not high and tends to decrease with increasing soaking time [Fig. 6(d)], which was in agreement with the change in alumina contents of mullites and second phase content in the 76/24 samples (Figs. 3 and 4). Both in the 74/26 and 76/24 samples, the mullite grains are always equiaxed.

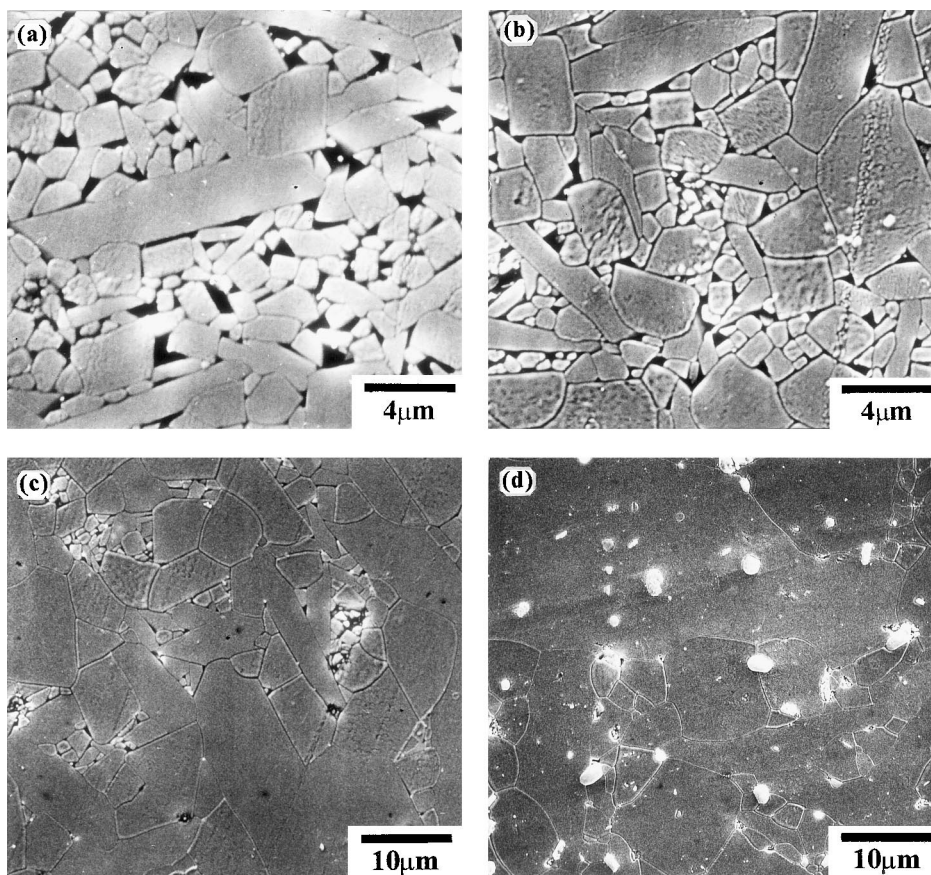


Fig. 9. Scanning electron micrographs of the samples (a) 68/32, (b) 71.8/28.2, (c) 74/26, and (d) 76/24, sintered at 1650°C for 4 h. Dark grains: mullite; light grains:  $\alpha$ -Al<sub>2</sub>O<sub>3</sub>.

The microstructures of the samples sintered at 1600 or 1650°C are shown in Figs. 8 and 9. It can be seen from Fig. 8 that the microstructures of the 68/32, 71.8/28.2, and 74/26 samples sintered at 1600°C did not change a lot compared with those sintered at 1550°C for 8 h, while the 76/24 sample sintered at 1600°C contained some fine alumina particles within equiaxed mullite grains in addition to the elongated  $\alpha$ -Al<sub>2</sub>O<sub>3</sub> grains, which were also observed at the lower temperature, on the boundaries of mullite grains. As sintering temperature increased to 1650°C, both elongated and rectangular mullite grains in the 68.32 and 71.8/28.2 samples became larger, fine mullite grains and large elongated mullite grains coexisted together with some pores in 74/26 sample (Fig. 9). In the 76/24 sample, some mullite grains became elongated and more  $\alpha$ -Al<sub>2</sub>O<sub>3</sub> grains were observed within mullite grains, which indicate that the mullite grain growth rate at above 1600°C was so high that alumina particles could not impede mullite boundary migration [Fig. 9(d)].

In ceramics with relatively low overall alumina contents (i.e. high silica contents), liquid phase would form and therefore large elongated and rectangular mullite grains were developed. As the overall alumina content of the samples increased, the morphology of mullite grains gradually changed to yield an equiaxed grain structure with alumina overall compositions  $\geq 74$  wt% Al<sub>2</sub>O<sub>3</sub>. Based on comparisons of SEM micrographs and alumina contents of mullite, the intrinsic growth rates of mullite crystal are believed not to be a function of composition, because both the 68/32 sample sintered at 1550°C for 8 h and the 76/24 sample sintered at the same temperature for 4 h had similar alumina contents of mullite. In 68/32 sample, elongated mullite grains were observed, while the morphology of mullite grains in 76/24 sample was equiaxed. In the samples with anisotropic mullite grains, elongated mullite grains were always accompanied with a number of fine mullite grains, and with increasing sintering temperature or time, the more elongated grains, the less fine grains can be formed, which is in agreement with that reported by Hong [7,8]. These results indicate that elongated mullite grains grow at the expense of the surrounding smaller grains. Fine grains have a large driving force for grain growth and promote the preferential growth of mullite along its *c*-axis by coalescence of the surrounding fine grains to yield an anisotropic grain microstructure [7].

#### 4. Conclusions

The mullite formation, densification behavior, and resulting microstructure of diphasic mullite gels were studied over a composition range from silica-rich to alumina-rich. Mullite formation initiated at about 1300°C for all samples. The alumina contents of mullite

grains in the samples sintered at high temperature (1650°C) for 4 h or at low temperature (1550°C) for longer time increased with the increase in alumina/silica ratio of the gels. A sharp decrease in densification rate was observed on transition from the mullite + silica-rich liquid phase field to the mullite solid solution. This decrease was associated with the elimination of viscous flow of the amorphous phase. However, the densification rate was higher for the samples with excess alumina than for the 74/26 sample near the boundary between the mullite solid solution range and the mullite + alumina phase region. Both in the rich-silica sample (68/32) and the stoichiometric mullite sample (71.8/28.2), elongated mullite grains were observed. Such elongated grains grew at the expense of the surrounding smaller mullite grains. In the 74/26 and 76/24 samples, mullite grains were equiaxed. When the alumina/silica ratio reached 76/24, some elongated  $\alpha$ -Al<sub>2</sub>O<sub>3</sub> grains formed in microstructure. These elongated alumina grains might be possible for the toughening of mullite ceramics.

#### References

- [1] I.A. Aksay, D.M. Dabbs, M. Sarikaya, Mullite for structural, electronic, and optical application, *J. Am. Ceram. Soc.* 74 (1991) 2343–2358.
- [2] P.A. Lessing, R.S. Gordon, K.S. Mazdiyasn, Creep of polycrystalline mullite, *J. Am. Ceram. Soc.* 58 (1975) 149–154.
- [3] B. Sonuparlak, Sol–gel processing of infrared-transparent mullite, *Adv. Ceram. Mater.* 3 (1988) 263–267.
- [4] G.S. Perry, Microwave dielectric properties of mullite, *Trans. Brit. Ceram. Soc.* 72 (1973) 279–283.
- [5] J.A. Pask, X.W. Zhang, A.P. Tomsia, B.E. Yoldas, Effect of sol–gel mixing on mullite microstructure and phase equilibria in the  $\alpha$ -Al<sub>2</sub>O<sub>3</sub>–SiO<sub>2</sub> system, *J. Am. Ceram. Soc.* 70 (1987) 704–707.
- [6] T.J. Mroz, J.W. Laughner, Microstructures of mullite sintered from seeded sol–gels, *J. Am. Ceram. Soc.* 72 (1989) 508–509.
- [7] S.-H. Hong, W. Cermignani, G.L. Messing, Anisotropic grain growth in seeded and B<sub>2</sub>O<sub>3</sub>-doped diphasic mullite gels, *J. Eur. Ceram. Soc.* 16 (1996) 133–141.
- [8] S.-H. Hong, G.L. Messing, Anisotropic grain growth in diphasic-gel-derived titania-doped mullite, *J. Am. Ceram. Soc.* 81 (1998) 1269–1277.
- [9] H. Schneider, Transition metal distribution in mullite, in: S. Davis, R.F. Davis, J.A. Pask (Eds.), *Ceramic Transactions*, Vol. 6, Mullite and Mullite Matrix Composites, The American Ceramic Society, Westerville, OH, 1990, pp. 135–158.
- [10] M.G.U. Ismail, H. Arai, Z. Nakai, T. Akiba, Mullite whiskers from precursor gel powders, *J. Am. Ceram. Soc.* 73 (1990) 2736–2739.
- [11] M.D. Sacks, J.A. Pask, Sintering of mullite-containing materials: I, effect of composition, *J. Am. Ceram. Soc.* 6 (1982) 65–70.
- [12] M. Ohashi, H. Tabata, O. Abe, S. Kanzaki, S. Mitachi, T. Kumazawa, Preparation of translucent mullite ceramics, *J. Mater. Sci. Lett.* 6 (1987) 528–530.
- [13] D.X. Li, W.J. Thomson, Mullite formation from nonstoichiometric diphasic precursors, *J. Am. Ceram. Soc.* 74 (1991) 2382–2387.
- [14] M. Zhou, J.M.F. Ferreira, A.T. Fonseca, J.L. Baptista, In situ formed  $\alpha$ -alumina platelets in a mullite–alumina composite, *J. Eur. Ceram. Soc.* 18 (1998) 495–500.

- [15] D. Michel, L. Mazerolles, R. Portier, Directional solidification in the alumina-silica system microstructure and interfaces, *Ceram. Trans.* 6 (1990) 435–447.
- [16] K. Okada, N. Otuska, Synthesis of mullite whiskers and their application in composites, *J. Am. Ceram. Soc.* 74 (1991) 2414–2418.
- [17] J.-S. Ha, K.K. Chawla, The effect of precursor characteristics on the crystallization and densification of diphasic mullite gels, *Ceram. Int.* 19 (1993) 299–305.
- [18] D.-Y. Jeng, M.M. Rahaman, Sintering and crystallization of mullite powder prepared by sol-gel processin, *J. Mater. Sci.* 28 (1993) 4904–4909.
- [19] F. Kara, J.A. Little, Sintering of pre-mullite powder obtained by chemical processing, *J. Mater. Sci.* 28 (1993) 1323–1326.
- [20] B. Saruhan, U. Voß, H. Schneider, Solid-solution range of mullite up to 1800°C and microstructural development of ceramics, *J. Mater. Sci.* 29 (1994) 3261–3268.
- [20] M.I. Osendi, P. Miranzo, Thermal evolution and sintering behavior of a 2:1 mullite gel, *J. Am. Ceram. Soc.* 80 (1997) 1573–1578.
- [22] S. Aramaki, R. Roy, Revised phase diagram for the system  $\text{Al}_2\text{O}_3\text{--SiO}_2$ , *J. Am. Ceram. Soc.* 45 (1962) 229–242.
- [23] R.F. Davis, J.A. Pask, Diffusion and reaction studies in the system  $\text{Al}_2\text{O}_3\text{--SiO}_2$ , *J. Am. Ceram. Soc.* 5 (1972) 525–531.
- [24] I.A. Aksay, J.A. Pask, Stable and metastable equilibria in the system  $\text{SiO}_2\text{--Al}_2\text{O}_3$ , *J. Am. Ceram. Soc.* 58 (1975) 507–512.
- [25] F.J. Klug, S. Prochazka, R.H. Doremus,  $\text{Al}_2\text{O}_3\text{--SiO}_2$  system in the mullite region, *J. Am. Ceram. Soc.* 70 (1987) 750–759.
- [26] M.I. Osendi, C. Baudin, S. de Aza, J.S. Moya, Processing and sintering of a 3:2 alumina-silica gel, *Ceram. Int.* 18 (1992) 365–372.
- [27] W.-C. Wei, J.W. Halloran, Phase transformation of diphasic aluminosilicate gels, *J. Am. Ceram. Soc.* 71 (1988) 166–172.
- [28] W.-C. Wei, J.W. Halloran, Transformation kinetics of diphasic aluminum silicate gels, *J. Am. Ceram. Soc.* 71 (1988) 581–587.
- [29] S. Sundaresan, I.A. Aksay, Mullitization of diphasic aluminosilicate gels, *J. Am. Ceram. Soc.* 74 (1991) 2388–2392.
- [30] W.E. Cameron, Composition and cell dimensions of mullite, *J. Am. Ceram. Soc.* 56 (1977) 1003–1007.
- [31] M.G.M.U. Ismail, Z. Nakai, S. Somiya, Microstructure and mechanical properties of mullite prepared by the sol-gel method, *J. Am. Ceram. Soc.* 70 (1987) C7.